Single and double acceptor-levels of a carbon-hydrogen defect in n-type silicon

R. Stübner, L. Scheffler, Vl. Kolkovsky,[a] and J. Weber
Technische Universität Dresden, 01062 Dresden, Germany

(Received 26 February 2016; accepted 13 May 2016; published online 27 May 2016)

In the present study, we discuss the origin of two dominant deep levels (E42 and E262) observed in *n*-type Si, which is subjected to hydrogenation by wet chemical etching or a dc H-plasma treatment. Their activation enthalpies determined from Laplace deep level transient spectroscopy measurements are E_C-0.06 eV (E42) and E_C-0.51 eV (E262). The similar annealing behavior and identical depth profiles of E42 and E262 correlate them with two different charge states of the same defect. E262 is attributed to a single acceptor state due to the absence of the Poole-Frenkel effect and the lack of a capture barrier for electrons. The emission rate of E42 shows a characteristic enhancement with the electric field, which is consistent with the assignment to a double acceptor state. In samples with different carbon and hydrogen content, the depth profiles of E262 can be explained by a defect with one H-atom and one C-atom. From a comparison with earlier calculations [Andersen *et al.*, Phys. Rev. B **66**, 235205 (2002)], we attribute E42 to the double acceptor and E262 to the single acceptor state of the CH_{1AB} configuration, where one H atom is directly bound to carbon in the anti-bonding position. *Published by AIP Publishing.*
[http://dx.doi.org/10.1063/1.4952702]

INTRODUCTION

Heat treatment of Si wafers in hydrogen (H) containing atmospheres is an important step in modern microelectronics to passivate the electrical activity of interface and surface states.[1,2] However, often additional processing of the samples leads to indiffusion of hydrogen into the bulk of the wafer and the interaction of H with various crystal imperfections. Sometimes a complete passivation is detected or a creation of novel, electrically active defects in the band gap of Si.[3–6] Some of the H-related defects may act as strong recombination centres, which reduce the carrier lifetime in Si devices.[3–5] Therefore, an understanding of the electrical and structural properties of H-related impurities and their formation becomes important not only from the scientific point of view but also because of their importance for device function.

Substitutional carbon is an isoelectronic impurity in Si where it can be observed in standard Float-zone (*FZ*) or Czochralski-grown (*CZ*) wafers in concentrations of 10^{15}–10^{16} cm^{-3}. The interaction of carbon with hydrogen was found to generate carbon-hydrogen (CH) complexes in *n*- and *p*-type Si.[7–12] According to theory, five different defect structures consisting of a substitutional carbon atom and a single hydrogen atom were predicted.[7] The most stable configuration for the negative and positive charge states of this defect is a H-atom located in the bond-centred position between C and a neighbouring Si atom (CH_{1BC}). The positive charge state of CH_{2BC} (a H atom located between two silicon atoms neighbouring carbon) and the negative charge state of CH_{1AB} (H atom directly bond to carbon in the anti-bonding position) and CH_{1Td} (H atom located at the interstitial T_d position close to carbon) were predicted to be slightly less stable (around 0.1–0.2 eV) compared to CH_{1BC} in Si. Theory also predicted the level positions of the different CH structures. However, the experimental support given in Ref. 7 was far from satisfying.

From deep level transient spectroscopy (DLTS) and Laplace DLTS studies, four different levels, labelled CH_A,[7,8] CH_B,[8] H180,[9] and $(CH)_I$[7] in the literature, were previously attributed to various CH-defects. The activation enthalpy of these defects was E_C-0.16 eV (CH_A), E_C-0.14 eV (CH_B), E_C-0.14 eV ($(CH)_I$), and E_V+0.33 eV (H180). The complexes CH_B,[8] $(CH)_I$,[7] and H180[9] were identified as single donor levels and CH_A as a single acceptor level from the change of the emission rates with electric field.[7,8] Depth profiles of CH_A[8] as well as uniaxial stress measurements[7] correlated this defect with CH_{1BC}. $(CH)_I$ was assigned to a CH-complex with a H atom in the bond-centred position located between the next and 2nd next Si atom of a substitutional carbon atom (CH_{2BC}).[7] This defect appears only after low temperature H implantation and anneals out already at 230 K. The CH_B complex is formed at about 320 K during annealing under reverse bias in the hydrogen rich region of a diode. A CH defect with more than one H atom was proposed as origin of the CH_B defect.[8] The nature of H180 is still under discussion. Slightly above room temperature, the levels CH_A, CH_B, and H180 anneal out. In the present study, we detect two additional electrical levels of the substitutional carbon-hydrogen complex in Si. The properties of the levels are determined and their origin will be discussed.

EXPERIMENTAL

Float-zone (*FZ*) and Czochralski (*CZ*) wafers from various vendors with different doping levels and different concentrations of carbon and oxygen are studied. The data for

[a]kolkov@ifpan.edu.pl

the wafers determined by *C-V* measurements and as given by the vendors are summarized in Table I together with the labelling of the samples. The wafers are cut into $10 \times 5\,mm^2$ samples and cleaned in acetone and di-ionized water. Hydrogen is introduced into the samples by wet chemical etching in CP4A ($HF:HNO_3:CH_3COOH$ 3:5:3) at room temperature or by a remote dc hydrogen-plasma at different temperatures of the samples. After the H-plasma treatment, the samples are dipped in HF and Schottky-contacts were fabricated by resistive evaporation of Au through a shadow mask onto the polished side of the sample. Ohmic contacts are made by rubbing eutectic InGa alloy onto the backside of the samples. The quality of the Schottky and Ohmic contacts is checked by current-voltage and capacitance-voltage (*C-V*) measurements at room temperature and at 50 K. The *C-V* curves are recorded at 1 MHz. Conventional DLTS and high-resolution Laplace DLTS are used to investigate the electrical properties of defects. The labelling of the DLTS lines in this work corresponds to the temperatures at which the peak positions were observed in the DLTS spectra at an emission rate of $50\,s^{-1}$.

The DLTS and Laplace DLTS signals are proportional to the capacitance changes ΔC caused by emission of carriers from the deep traps. Therefore, a direct comparison of the intensity of the peaks in the DLTS and Laplace DLTS spectra without calculating their concentrations is ambiguous, and it can lead to erroneous conclusions. Indeed, the doping level and the lambda-layer are not identical in differently hydrogenated samples. The shift of the probed region towards the bulk at low temperatures (for example, due to the freeze-out effect or due to relative large concentrations of deep level defects which compensate shallow donors in the near-surface region) could also result in a strong reduction of the intensity or even the absence of low temperature peaks.

The depth profiles of the defects are calculated from the Laplace DLTS spectra by taking into account the λ-layer.[13] The electric field is calculated from the *C-V* measurements as described in Ref. 13. Some samples are subjected to isochronal annealing steps of 60 min in air.

RESULTS

Conventional DLTS spectra of the hydrogenated FZ1 sample are shown in Fig. 1. After wet chemical etching or H-plasma treatment performed at a sample temperature of 323 K, three DLTS peaks labelled E42, E90, and E262 are observed. The E90 peak is not detected in samples after a dc H-plasma treatment at temperatures above 373 K. Calculated concentrations from the DLTS intensities of E42, E90, and E262 are low (between 5×10^{10} and $10^{12}\,cm^{-3}$) after wet chemical etching in FZ1; therefore, these levels can be better detected in sample with lower free carrier concentrations (Fig. 2).

The DLTS spectra of sample CZ1 (Fig. 3) differ from those in the *FZ*-Si samples. In this sample, E90 and two additional peaks E75 and E65 (observed as a shoulder to E75) can be detected after wet chemical etching. These peaks also appear in samples hydrogenated by a dc H-plasma treatment. Similar to the FZ1 sample, E42 and E262 are present in the DLTS spectrum after a H-plasma treatment performed at different temperatures. The concentration of E42 and E262 increases if more H is introduced into the samples through a higher temperature of the H plasma treatment.[14]

TABLE I. List of samples used in this study. Phosphorous concentrations are obtained from our C-V measurements; substitutional carbon and interstitial oxygen concentrations are given by the vendors (CZ1 and CZ4 are samples from different vendors).

Sample	Phosphorous concentration (cm^{-3})	Substitutional carbon concentration (cm^{-3})	Interstitial oxygen concentration (cm^{-3})
FZ1	1×10^{15}	5×10^{15}	$<1 \times 10^{16}$
FZ2	1×10^{14}	5×10^{15}	$<1 \times 10^{16}$
FZ3	7×10^{14}	5×10^{15}	$<1 \times 10^{16}$
FZ4	2×10^{15}	5×10^{15}	5×10^{15}
CZ1	1×10^{15}	5×10^{15}	1×10^{18}
CZ2	5×10^{14}	5×10^{15}	6×10^{17}
CZ3	1×10^{14}	5×10^{15}	1×10^{18}
CZ4	1×10^{15}	5×10^{15}	1×10^{18}
CZ5	2×10^{15}	8×10^{16}	3×10^{17}

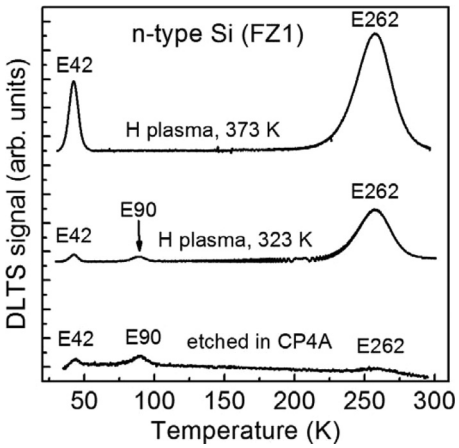

FIG. 1. Conventional DLTS spectra recorded in wafer FZ1. Samples were subjected to hydrogenation by wet chemical etching at room temperature or by H-plasma treatments with samples at temperatures of 323 K or 373 K. The spectra were recorded with the following parameters: $e_n = 50\,s^{-1}$, $V_R = -2$ V, $V_P = 0$ V, and $t_p = 1$ ms.

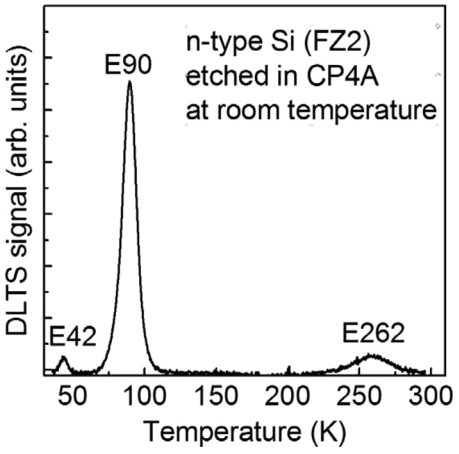

FIG. 2. Conventional DLTS spectrum recorded in wafer FZ2 after wet etching in CP4A. The spectra were recorded with the following parameters: $e_n = 50\,s^{-1}$, $V_R = -2$ V, $V_P = -0$ V, and $t_p = 1$ ms.

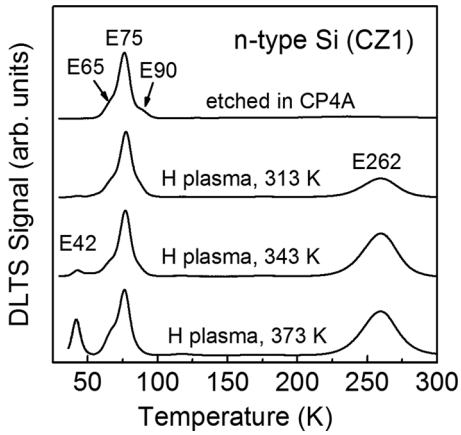

FIG. 3. Conventional DLTS spectra recorded in wafer CZ1. Samples were subjected to hydrogenation by wet chemical etching or by a H-plasma treatment with a sample temperature of 313 K, 343 K, or 373 K. The spectra were recorded with the following parameters: $e_n = 50\,s^{-1}$, $V_R = -3$ V, $V_P = 0$ V, and $t_p = 1$ ms.

In the following, we concentrate our attention on the discussion of the origin of the defects E42 and E262 which appear in both *FZ* and *CZ* Si after hydrogenation.

Figure 4 presents the Laplace DLTS spectra recorded at 46 K and at 266 K in sample FZ1 after H-plasma treatment performed at 373 K. Both spectra exhibit only one single Laplace DLTS peak. The Arrhenius plots of E42 and E262 are given in Fig. 5. These plots yield activation enthalpies of E_C-0.06 eV and E_C-0.51 eV and apparent capture cross sections of $\sigma_{na} = 2 \times 10^{-17}\,cm^2$ and $\sigma_{na} = 1.8 \times 10^{-15}\,cm^2$ for E42 and E262, respectively. The electric field is approximately the same (6500 V/cm) for both Laplace DLTS measurements. Defects with similar electrical properties as E42 and E262 have been previously reported in Refs. 15–17.

The emission rate for E262 is not enhanced with increasing electric field applied to the diode (Fig. 6). A direct measurement of the capture cross section at different temperatures does not yield a capture barrier for electrons for this defect. Therefore, we assign E262 to a single acceptor level. This assignment is supported by the results of Ref. 15. In contrast, the emission rate of E42 increases with electric field (Fig. 6, solid line). The enhancement is found to be significantly smaller compared to that expected for a defect with a

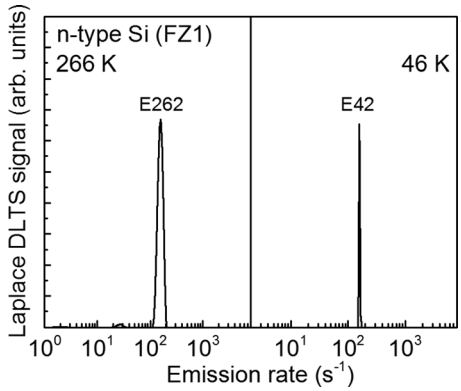

FIG. 4. Laplace DLTS spectra observed at 46 K and 266 K in *FZ*-silicon treated in a dc H-plasma at 373 K. The spectra were recorded with the following parameters: $V_R = -2.5$ V, $V_{P1} = -0$ V, $V_{P2} = -1$ V, and $t_p = 1$ ms.

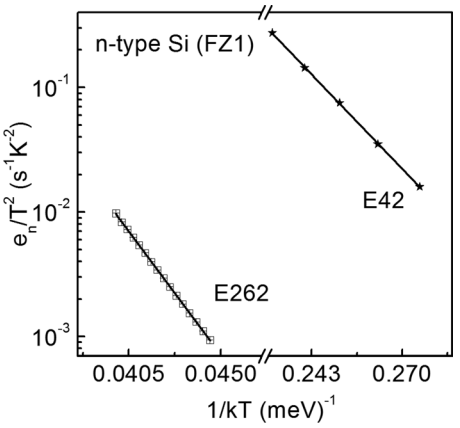

FIG. 5. Arrhenius plots of the levels observed in Fig. 4.

Coulombic potential in the frame of the Hartke model (three dimensional Poole-Frenkel effect)[18] (dashed line).

In order to describe the field dependence of the emission rate of E42 quantitatively, we use the model of a defect with a repulsive potential. In Ref. 19, the effect of a short-range repulsive potential superimposed on the Poole-Frenkel potential was investigated for the EL2 defect in *n*-type GaAs. The short-range repulsive potential was described by an inverted Morse potential. Beyond the short-range attractive potential, which defines the bound state of the defect, the authors suggested that a Morse potential could also approximate the repulsive Coulombic interaction between the emitted electron and a negatively charged center. Following this idea, we fit our experimental data with the repulsive potential from Ref. 19. The best correspondence between experimental data and theory is obtained for a width of the barrier of $\lambda = 1.6$ nm, a barrier height of $U_0 = 60$ meV, and an emission rate at zero field $e_{n0} = 22\,s^{-1}$ (solid line in Fig. 6).

The thermal stability of E42 and E262 in the hydrogen plasma treated sample FZ3 at 373 K is investigated by isochronal annealing steps of 60 min in air (Fig. 7). After each annealing step the concentration is calculated at the same depth of around 1.7 μm. The annealing behaviour of the defects is found to be identical within the accuracy of the

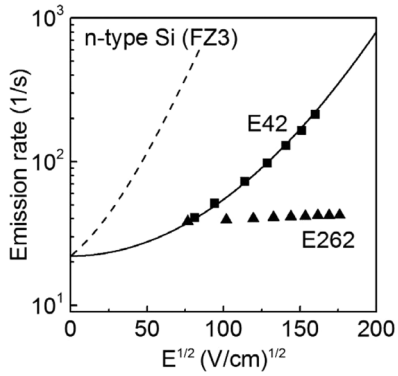

FIG. 6. Emission rate of E42 and E262 as a function of the square root of the electric field. The solid line shows the results of calculations for a defect having a repulsive potential. The dashed line presents the results of the calculation for a defect having a Coulombic attractive potential using the Poole-Frenkel model.

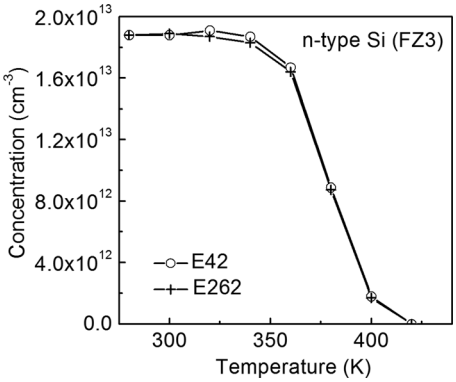

FIG. 7. Concentration changes of E42 and E262 as a function of annealing temperatures. The concentration of the defects was determined at the same depth of ~1.7 μm below the surface. The annealing time was 60 min. Sample FZ3 was treated in a hydrogen plasma at T = 373 K prior to the annealing.

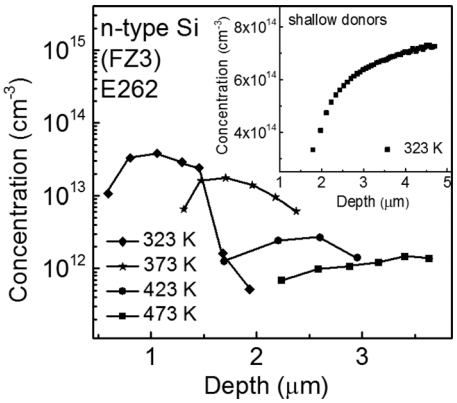

FIG. 9. Concentration depth profiles of E262 in FZ3 recorded after dc H plasma treatments at different temperatures. The inset shows the concentration of shallow donors after H plasma treatment at 323 K.

experiment. Their concentrations decrease by a factor of two at about 375 K, and they anneal out at about 420 K.

Depth profiles of E42, E90, and E262 recorded after wet chemical etching in the FZ2 sample are given in Fig. 8. These profiles are found to be identical for E42 and E262. The concentration of E90 is around 10 times higher compared to the concentrations of E42 and E262. However, the slope of the reduction of the concentration of E42, E90, and E262 is the same, as indicated by the solid lines in Fig. 8.

Depth profiles of E262 recorded in FZ3 after H-plasma treatment at different temperatures are compared in Fig. 9. With increasing temperature of the H-plasma treatment, the depth profiles shift deeper into the bulk. However, they are located in the same region where hydrogen passivated shallow donors (P-H), as determined by C-V measurements, are detected (inset in Fig. 9). As mentioned above, the shift of the probed region at low temperatures in some samples prevents the detection of E42 close to the surface, and therefore, it is not possible to compare the whole depth profiles of E42 and E262 in all samples investigated below. However, in the region where both E42 and E262 could be detected, the depth profiles are found to be always identical. Therefore, below we investigate the depth profiles of E262 in dependence of carbon, phosphorous, and oxygen, and similar conclusions can be drawn for E42.

In order to check whether E42 and E262 correlate with the phosphorous, oxygen, or carbon concentration, samples with different concentrations of O, C, and P are subjected to a H-plasma treatment at 323 K. Figure 10 presents depth profiles of E262 in samples CZ1, CZ2, and CZ3 with similar carbon and oxygen concentrations but different contents of shallow donors (phosphorous). A higher P concentration leads to a shift of the depth profile of E262 towards the surface. However, the maximum concentration of E262 is about 2×10^{13} cm^{-3} in all samples, which indicates that the corresponding defect does not contain P. We interpret the shift of the depth profiles as a result of a more effective capture of incoming H with P in samples which contain more shallow donors. The higher PH concentration leads to a reduction of hydrogen which can be trapped at carbon. Similar depth profiles for E262 are also obtained in samples doped with Sb and As.

Figure 11 presents the depth profiles of E262 recorded in samples with similar carbon concentrations but more than two orders of magnitude different O content (CZ4 and FZ4). The profiles are similar, and they verify that this defect does not contain oxygen. One should notice that the phosphorous concentration varies slightly in the samples CZ4 and FZ4 (see Table I). However, the concentration of E262 does not depend on the P concentration (Fig. 10), and as a result, the different P concentrations should not influence the conclusions drawn from Fig. 11.

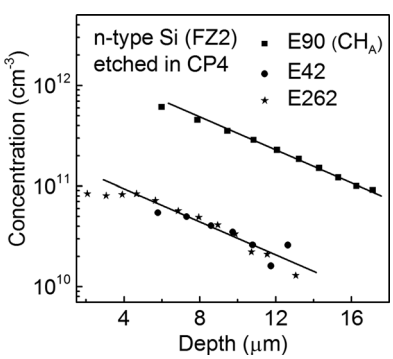

FIG. 8. Concentration depth profiles of E262, E42, and E90 recorded after wet etching in CP4A of sample FZ2. The solid lines indicate the same slope of the profiles.

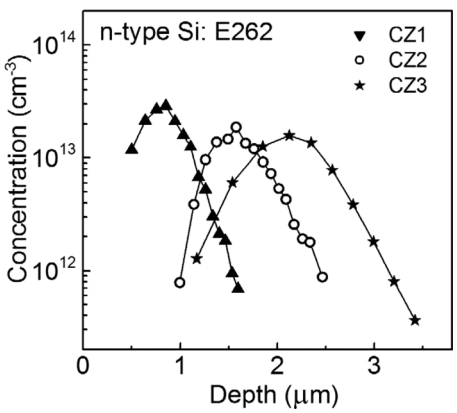

FIG. 10. Concentration depth profiles of E262 in H-plasma treated *n*-type *CZ*-Si samples for three different doping concentrations. The concentration of carbon and oxygen is similar in these samples.

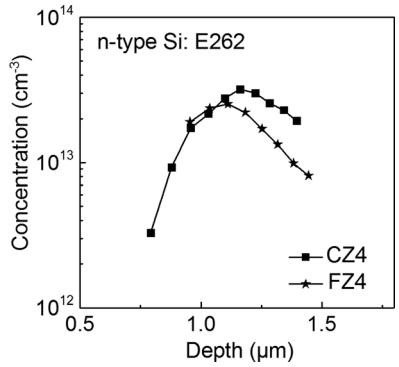

FIG. 11. Depth profiles of E262 from CZ4 and FZ4 hydrogenated in a dc H-plasma at 373 K. Samples have different oxygen concentrations but the same carbon concentration.

Figure 12 compares the depth profiles of samples (CZ4 and CZ5) containing different carbon concentrations. In the sample with higher C content of about $8 \times 10^{16}\,\mathrm{cm}^{-3}$ (CZ5), the concentration of E262 significantly exceeds that from the sample with a lower C content of about $5 \times 10^{15}\,\mathrm{cm}^{-3}$ (CZ4). In addition, the depth profiles of PH recorded in these samples are also presented in Fig. 12.

Several *FZ*-samples (from wafer FZ3) are treated in a dc H-plasma at 373 K. Afterwards, the samples are annealed under a reverse bias of −2 V at 320 K for 120 min (reverse bias annealing (RBA)). The depth profiles of E262 are found to be identical before and after RBA (Fig. 13). In contrast, the same annealing conditions shift the depth profile of E90 towards the bulk with a concentration maximum close to the end of the depletion region during RBA (marked by the dashed line).

DISCUSSION

In Ref. 8, two different CH-related defects (CH_A and CH_B) with very close level positions were shown to appear in the depletion region of hydrogenated C-doped Si before (CH_A) and after RBA (CH_B). CH_A was correlated with the single acceptor state of the CH complex where H is located in the bond-centred position between a Si atom and a neighbouring C atom (CH_{IBC}),[7] whereas CH_B was assigned to the single donor state of a defect containing more H atoms compared to CH_A.[8] A comparison of the DLTS peaks from

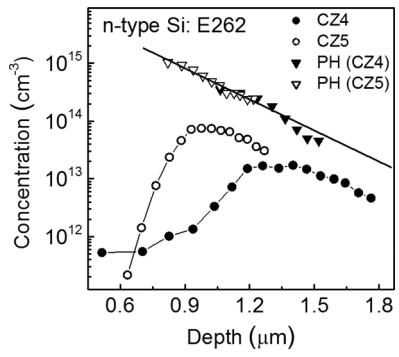

FIG. 12. Depth profiles of E262 and PH from CZ4 and CZ5 hydrogenated in a dc H-plasma at 323 K.

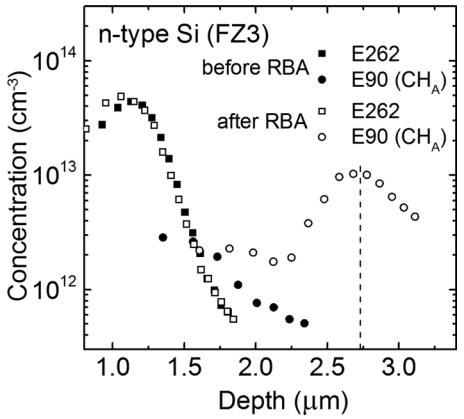

FIG. 13. Depth profiles of E90 and E262 before and after RBA (−2 V at 320 K for 120 min). Sample FZ3 was first hydrogenated in a dc H-plasma at 323 K. The broken line shows the end of the depletion region for the bias applied during the RBA treatment.

Fig. 1 and their electrical properties with literature data allows us to correlate the E90 level observed in this study with the CH_A defect.

The thermal stability and the electrical fingerprints of E65 and E75 agree well with those reported in Refs. 20 and 21. Similar to the results of our studies, E65 and E75 were previously observed only in *CZ*-Si and attributed to different charge states of COH-defects.[20]

The identical depth profiles for E42 and E262 and their similar annealing behaviour relate these two levels to the same defect. This defect contains hydrogen since its concentration increases with the H concentration, and it is located in the same region where a passivation of shallow donors by H was observed.

Feklisova and Yarykin[22] showed that the concentration of hydrogen-related defects introduced by wet chemical etching decreased towards the bulk. The slope of this decrease is proportional to exp(-*ix*/*L*), where *i* is the number of hydrogen atoms in the complex and *L* is the penetration depth of the hydrogen species. Therefore, if one compares the concentration of different hydrogen-related defects as a function of depth, the number of hydrogen atoms in these complexes can be directly derived. As shown in Fig. 8, the slope of the concentration profile of E42 and E262 is identical to that of E90. In accordance with the results of Ref. 22, the defect with the levels E42 and E262 should also contain only one H atom similar to E90.

As mentioned above, we attribute E42 to the double acceptor state and E262 to the single acceptor state in *n*-type Si. This assignment is consistent with the factor of 10 smaller apparent capture cross section of E42 compared to that of E262.

In contrast to our findings, Johnson *et al.*[15] reported no enhancement of the emission rate for E42. However, due to the weak electric field (below 3000 V/cm) used in Ref. 15, the changes of the emission rate of E42 were not detectable (see Fig. 6).

Both E42 and E262 are found deep below the sample surface, and they do not originate from electrically active surface states created by the hydrogenation or from hydrogen

platelets. We also rule out that unintentionally introduced impurities such as transition metals (TMs) are responsible for these defects. E42 and E262 are observed in different samples with various doping densities and without any detectable traces of TM impurities. Depth profiles recorded in samples with different C concentrations (Fig. 12) show a clear dependence on the C content in the samples. However, it is not possible to obtain a one-to-one correlation between the concentrations of carbon and E262 because of the different content of H at different depths as obtained from the PH profiles (Fig. 12). In this case, H acts as a limiting factor for the formation of the E262 defect.

The correlation of E262 and E42 with carbon and one hydrogen atom suggests that these defects belong to different charge states of a CH-related defect. Taking into account that the concentration of carbon varies only from 5×10^{15} to $8 \times 10^{16}\,\mathrm{cm}^{-3}$ in our samples, the probability of having two carbon atoms close to each other is rather low. Therefore, it is reasonable to assign E42 and E262 to the double acceptor and the single acceptor of a CH-related complex with only one C and one H atom, respectively. As mentioned above, the depth profiles of E262 are identical before and after RBA performed at 320 K, and we did not detect any transformation between CH_A and E262 (E42). However, one should remember that annealing at 340–350 K also results in the dissociation of the PH complex in *n*-type Si. Due to the dissociation of the complex, free H atoms drift towards the bulk under the RBA annealing conditions. The comparison of CH_A and E42 (E262) in as-grown and annealed samples becomes impossible since different regions in the sample are being compared. Moreover, the interaction between positively charged P and negatively charged H atoms is more efficient compared to that between H^- and neutral C species.

In accordance with the results of the calculations of Ref. 7, the energy of the negative charge state of the CH_{1AB} configuration should be only around 0.2 eV higher compared to CH_{1BC}. The single acceptor CH_{1AB} was predicted to introduce a deep level with an activation energy of 0.63 eV below the conduction band. Taking into account a possible error in the calculated level position of the defects, the activation enthalpy of E262 (about 0.51 eV) satisfactorily agrees to that predicted for CH_{1AB} in Ref. 7. In this case, the E42 level is then related to the double acceptor state of the CH_{1AB} defect.

The E42 and E262 levels were also observed in *CZ*-Si where the concentration of CH_{1BC} was relatively small. In addition to CH_{1BC}, two other defects E65 and E75 with higher concentrations appeared in the DLTS spectrum. It seems reasonable to suggest that the CO complex, which is electrically inactive in *CZ*-Si, interacts efficiently with hydrogen in hydrogenated samples leading to the formation of COH-complexes which were previously correlated with E65 and E75.[20] In contrast, the low concentration of oxygen in *FZ*-Si results in the efficient interaction of carbon and hydrogen which results in a larger concentration of CH_{1BC}.

A schematic diagram of the CH-related levels, which were observed in the present study, and their defect assignments are present in Fig. 14.

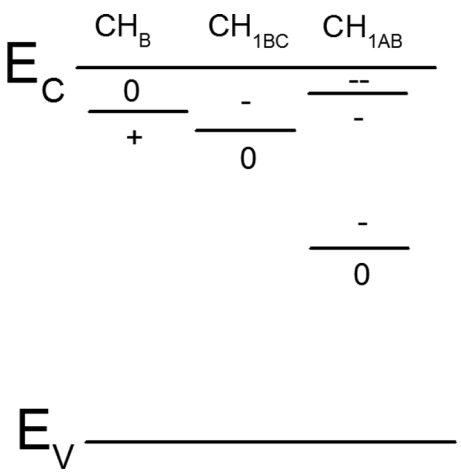

FIG. 14. Schematic level positions of the studied CH-defects.

SUMMARY

Two DLTS peaks E42 and E262 are observed in *n*-type *FZ*- and *CZ*-Si after hydrogenation by wet chemical etching or dc H-plasma treatment. The annealing behaviour and the depth profiles of these defects demonstrate that E42 and E262 are different charge states of the same defect. Depth profiles of E42 and E262 directly after wet-chemical etching as well as a comparison of the defect concentrations in different samples suggest a defect structure with one hydrogen and one carbon atom. Due to the absence of the Poole-Frenkel effect and the lack of a capture barrier for electrons, we assign E262 to a single acceptor state. The enhancement of the emission rate of E42 is well described by a model of a double acceptor level with a repulsive potential. The properties of E42 and E262 correlate well with the calculated CH_{1AB} configuration where the H atom is bonded directly to substitutional carbon in the anti-bonding position.

[1]J. I. Pankove, D. E. Carlson, J. E. Berkeyheiser, and R. O. Wance, Phys. Rev. Lett. **51**, 2224 (1983).
[2]C. T. Sah, Y.-C. J. Sun, and J.-T. J. Tzou, Appl. Phys. Lett. **43**, 204 (1983).
[3]A. R. Peaker, V. P. Markevich, and L. Dobaczewski, "Hydrogen related defects in silicon, germanium and silicon-germanium alloys," in *Defects in Microelectronic Materials and Devices*, edited by D. M. Fleetwood, S. T. Pantelides, and R. D. Schrimpf. (Taylor and Francis, New York, 2008).
[4]S. K. Estreicher, M. Stavola, and J. Weber, "Hydrogen in Si and Ge," *Silicon, Germanium, and Their Alloys*, edited by G. Kissinger and S. Pizzini (Taylor and Francis, New York, 2014).
[5]L. Scheffler, Vl. Kolkovsky, and J. Weber, J. Appl. Phys. **117**, 085707 (2015).
[6]L. Scheffler, Vl. Kolkovsky, and J. Weber, J. Appl. Phys. **116**, 173704 (2014).
[7]O. Andersen, A. R. Peaker, L. Dobaczewski, K. Bonde Nielsen, B. Hourahine, R. Jones, P. R. Briddon, and S. Öberg, Phys. Rev. B **66**, 235205 (2002).
[8]R. Stübner, Vl. Kolkovsky, and J. Weber, J. Appl. Phys. **118**, 055704 (2015).
[9]Y. Kamiura, M. Tsutsue, Y. Yamashita, F. Hashimoto, and K. Okuno, J. Appl. Phys. **78**, 4478 (1995).
[10]A. Endrös, Phys. Rev. Lett. **63**, 70–73 (1989).
[11]A. L. Endrös, W. Krühler, and F. Koch, J. Appl. Phys. **72**, 2264–2271 (1992).
[12]W. Csaszar and A. L. Endrös, Phys. Rev. Lett. **73**, 312–315 (1994).
[13]P. Blood and P. W. Orton, *The Electrical Characterization of Semiconductors: Majority Carriers and Electron States* (Academic Press, 1992).

[14]S. J. Pearton, J. W. Corbett, and M. Stavola, *Hydrogen in Crystalline Semiconductors* (Springer, 1992).
[15]N. M. Johnson, F. A. Ponce, R. A. Street, and R. J. Nemanich, Phys. Rev. B **35**, 4166 (1987).
[16]Y. L. Huang, E. Simoen, C. Claeys, J. M. Rafi, and P. Clauws, J. Mater. Sci.: Mater. Electron. **18**, 705 (2007).
[17]S. J. Pearton, J. M. Kahn, and E. E. Haller, J. Electron. Mater. **12**, 1003 (1983).
[18]J. L. Hartke, J. Appl. Phys. **39**, 4871 (1968).
[19]W. R. Buchwald and N. M. Johnson, J. Appl. Phys. **64**, 958 (1988).
[20]Y. Tokuda, I. Katoh, H. Ohshima, and T. Hattori, Semicond. Sci. Technol. **9**, 1733 (1994).
[21]M. Yoneta, Y. Kamiura, and F. Hashimoto, J. Appl. Phys. **70**, 1295 (1991).
[22]O. Feklisova and N. Yarykin, Semicond. Sci. Technol. **12**, 742 (1997).